JJMS **17**, No. 3, 401-412 (2024)

Jordan Journal of Mathematics and Statistics.
Yarmouk University

DOI:https://doi.org/10.47013/17.3.7

PERISTALSIS OF ELECTRO-OSMOTIC JEFFREY FLUID IN THE PRESENCE OF THERMAL RADIATION AND HEAT TRANSFER WITH THE PERMEABLE WALL

MAHADEV M CHANNAKOTE[1,*], *SHEKAR M*[2]

[1] Department of Mathematics and Statistics, M. S. Ramaiah University of Applied Science, Bengaluru, Karnataka 560054, India
[2] Department of Mathematics, B.M.S. College of Engineering, Bengaluru, Karnataka 560019, India

Received: June 6, 2023 Accepted : Nov. 13, 2023

Abstract: The electro kinetic movement of fluids through microchannel and micro-peristaltic transport has raised concerns in the field of improved medical technology and various areas of biomedical science. In light of this, the electro-osmotic impact on the peristaltic flow of a Jeffrey fluid (ionic solution) in a microchannel with a permeable wall is investigated. To analytically solve the governing equations of the modulated problem, we make the assumptions of a long wavelength ($\delta \leq 0$) and a low Reynolds number($R_e \to 0$). The modelling also includes an analysis of the impacts of thermal radiation and heat transfer. In order to investigate the electro-kinetic mechanism, the Poisson-Boltzmann equation is analyzed, taking into account the zeta potential. The obtained set of dimensionless expressions is solved using Mathematica software. The effects of various parameters on flow deliveries are confirmed through plots. The analysis presented here may be helpful in examining the features of bio fluids and can initiate their movement through the application of an external electric field. The main findings demonstrate that electro osmosis plays a key role in regulating heat transfer as well as flow. Furthermore, this study holds potential implications across various disciplines including design, hematology, electrophoresis, and the enhancement of bio-mimetic electro-osmotic pumps

Keywords: Zeta potential; Permeable wall; Heat transfer; Thermal radiation; Electrical double laye.

2010 Mathematics Subject Classification. 76Z99; 76W99.

1 Introduction

The propagation of waves along the deformable walls of a channel results in peristaltic flows. Peristaltic transport is widely used in industrial peristaltic pumping due to its effective, clean, and safe method of fluid transfer, as it does not involve any internal moving components. This method is commonly used to drive blood through small blood vessels or artificial blood services for physiological and medicinal purposes. The mathematical study of peristaltic transport was first explored by Fung and Yih [1] and Shapiro et al. [2], who used the Navier-Stokes equations as model equations for a viscous fluid. Many researchers have since adopted this concept and applied it in situations where the pumped fluid must remain uncontaminated (e.g., blood) or non-corrosive, and should not come into contact with the working components of typical pumping devices. Peristaltic motion has been found to contribute to continuous regeneration. Additionally, peristaltic pumping is observed in various real-world biomechanical systems, including the heart-lung machine and various pumps. Recent studies ([3]-[10]) have presented this approach to examine peristaltic transport under various flow configurations with different geometries.

The study of bioheat transfer has attracted many investigators owing to its application in thermo-therapy and human thermoregulation system. Currently bioheat transfer is considered as a heat transfer in human body. Understanding fluid dynamics in the context of modeling biological liquids is greatly enhanced by studying the properties of heat transfer. Conduction, radiation, convection, and evaporation are some of the heat transfer methods that the body uses to maintain equilibrium. These mechanisms rely on the transfer of heat from one area to another. So, the rate at which heat exchange mechanisms operate varies depending on the ambient temperature and conditions. Vajravelu et al. [11] conducted a study

* Corresponding author e-mail: mchannakote@rediffmail.com

on the heat transfer properties of the peristaltic mechanism through a porous annulus in response to application. Recent research has also investigated the interaction between peristalsis, heat, and mass transfer during chemical reactions. Applications in this field include the oxygenation process, hemodialysis, blood flow convection from tissue pores, and diffusion of nutrients into the blood. As a result, several investigators ([12]–[17]) have reported on the analysis of the interaction between heat and peristalsis with various fluids. In a recent study, Mahadev and Dilipkumar [18] examined the effect of heat on the peristaltic activity of Rabinowitsch fluid through a porous medium. They also explored the consequences of convective and viscous dissipation on the peristaltic motion of an Ellis fluid with wall properties [19].

Thermal radiation plays a crucial role in many high-temperature processes, such as furnaces, boilers, and engine cooling techniques. Various manufacturing sectors have issued tenders for the design of nuclear power stations, utilizing this concept. In a study conducted by Rafiq and Abbas [20], the effects of thermal radiation and viscous dissipation on the peristaltic flow of Rabinowitsch viscoelastic fluid through a non-uniform tube were examined. They found that the Brinkman number is responsible for the properties of viscous dissipation, which helps increase the liquid temperature in all scenarios. Sunitha and Asha [21] investigated the impact of heat radiation on the peristaltic blood motion of a Jeffrey liquid involving double diffusion with gold nanoparticles. Hayat et al. [22] clarified the flow of magneto nanofluid in a porous channel using radiative peristaltic flow and thermal radiation. Naveed et al. [23] studied the effects of heat radiation and heterogeneous-homogeneous processes on the peristaltic flow of the Rabinowitsch fluid model. The impact of convective conditions on the physiological transport of the Rabinowitsch fluid model was examined by Hina Sadaf and Iqra Shahzadi [24]. Kothandapani and Prakash Jayavel [25] investigated the peristaltic movement of Williamson nanofluids in a tapered, asymmetric channel, which was influenced by the interaction between a heat radiation parameter and a magnetic field.

The study of electric fields and their interaction with fluid particles is of great interest to scientists. One particularly useful mechanism is electro-osmotic flow, which enables efficient micro-pumping in microchannels. This phenomenon, known as electro-osmosis, is caused by the Coulomb force and is influenced by the electric potential in the microchannel. Electroosmotic pumping, including valve-less switching and precise control of transportation and manipulation of liquid samples, takes advantage of this phenomenon. This makes electro-osmosis a preferred method for moving liquids in microfluidics, as it does not require any solid moving parts.

The current models also incorporate bio microfluidics, which focuses on studying biofluids in micro vessels. Due to its numerous applications in biomedical engineering and research, bio microfluidics has gained significant attention in recent years. Scientists have utilized electrokinetic phenomena to effectively manipulate and control fluid flow in micro vessels within microfluidics. Microfluidic devices have proven to be useful in analyzing biofluids, particularly in DNA concatenation, species separation, and fluid amalgamation, making them valuable in examining various biological processes. Motivated by the wide range of applications in biomedical engineering, there has been interest in mathematical simulations of peristaltic transport in microfluidic devices. Chakraborty [26] investigated the enhancement of peristaltic transport using electro osmosis, with a focus on Newtonian fluids. However, this model provides a straightforward formulation for assessing electro-peristaltic transport. The combination of the electro-osmotic mechanism with peristalsis in various channels has attracted significant attention from researchers worldwide. Recent studies have analyzed the electro-peristaltic transport of both Newtonian and Non-Newtonian fluids in different channels, as documented in several publications ([27]–[34]).

Another aspect of the current model involves the utilization of the electro-osmosis in porous media technique. This technique finds application in various fields such as coating processes, geothermal engineering, environmental engineering, rubber processing, and ceramic technology. Additionally, this method effectively eliminates the accumulated toxic heavy metal ions, which pose significant health and environmental risks. Many academics have explored the use of generalized Darcy's law for peristaltic flow across porous media. Electrophoresis in porous media plays a crucial role in various applications such as coating processes, geothermal engineering, environmental engineering, rubber processing, and ceramic technology. A few attempts at studying this phenomenon can be found in the available reference list ([35]–[44]).

Zeta potential (ZP) is a crucial physical property that governs electrostatic interactions in particle dispersions and plays a vital role in comprehending the stability of colloidal dispersions. There is a direct correlation between the charge on the capillary and the zeta potential (ξ), which is the potential resulting from the double layer on the capillary wall. The mobility and velocity of the EOF are highly dependent on pH because the zeta potential changes in response to variations in the capillary's charge. At high pH values, the silanol groups deprotonate, leading to an increase in the net charge of the capillary wall. A low zeta potential value (less than 30 mV) indicates potential issues such as flocculation, coagulation, aggregation, or instability. Several factors, including pH, temperature, instability radiation, concentration, ionic strength of the solution, and the composition of surface ligands, can influence the stability of wound-dressing materials. These variables need to be carefully considered.

Considering the extensive application of the electro-osmosis technique in porous media within the fields of geo-environmental and bio-environmental sciences, it is imperative to adopt this mindset. Numerous significant physiological studies have extensively demonstrated the electrohydrodynamic properties of blood. Furthermore, it is widely recognized that understanding the issue of heat and thermal radiation in the context of electro-osmosis via

peristalsis is crucial for advancing our knowledge in physiology and biomedicine. This becomes particularly valuable when examining the intricate processes involved in heat transfer within human tissues, including heat conduction in tissue, heat transfer from arterial venous blood perfusion through tissue pores, and the utilization of lab-on-chip systems in diagnostics. In these scenarios, it is imperative to investigate fluid behavior and potentially induce their movement through an external electric field. Electro-osmotic pumps offer the advantage of generating high pressure and flow rates without the need for mechanical components.

In light of the demonstrated effectiveness of various factors discussed earlier, our study aims to examine the influence of thermal radiation, heat transfer, zeta potential, and electro-osmotic effects on the peristaltic motion of the Jeffrey fluid within a channel with a permeable wall. Given the lack of prior research on the peristaltic flow of Jeffrey fluid through a (porous media) permeable wall under the influence of heat, thermal radiation, and electro-osmotic effects, this analysis is being undertaken. In this complex flow structure, we will examine the implications of fluid rheology, the influence of the Saffamann boundary condition on controlling variables, the effects of Helmholtz-Smoluchowski velocity, and the impact of the Debye length. The findings will be presented graphically and accompanied by analytical solutions. The findings of the ongoing investigation would greatly enhance the performance of bio microfluidic devices and contribute to the development of more comprehensive models.

1.1 Highlights and Novelties

1.Mathematical modeling for electro osmosis modulated the peristaltic flow of Jeffrey fluid through a channel with combined effects of heat and thermal radiation is taken into account.
2.Saffamann boundary condition and Zeta potential is considered for the system.
3.Debye-Hükel linearization approximation is considered to modify the electrodynamic problem.
4.Exact solutions to the problematic issue are computed and the key characteristics of biological problems are explored.
5.The current mathematical analysis has uses in lab-on-chip systems for medical diagnosis, where biofluids are examined and their transit can be triggered by an external electric field. The current findings offer a substantial foundation for analyzing experiments and developing more comprehensive models of microvascular blood flow.

2 Mathematical Formulation

2.1 Flow Analysis

The geometric model of the bioheat transfer and electroosmotic peristaltic flow of an incompressible viscoelastic fluid in the current study is illustrated in Fig. 1. We consider the electroosmotic flow of Jeffrey fluid (aqueous ionic solution) through a two-dimensional channel of finite length (L) and uniform thickness of ($2a$). Motion is generated due to propagation of infinite wave train travelling along the channel wall with velocity c. The electro-osmotic flow occurs by the applied external electric field E_x that flows parallel to the channel walls. As a result, the channel experiences electro-osmotic flow (EOF) as the positive (cations) and negative (anions) ions form the electrical double layer (EDL).

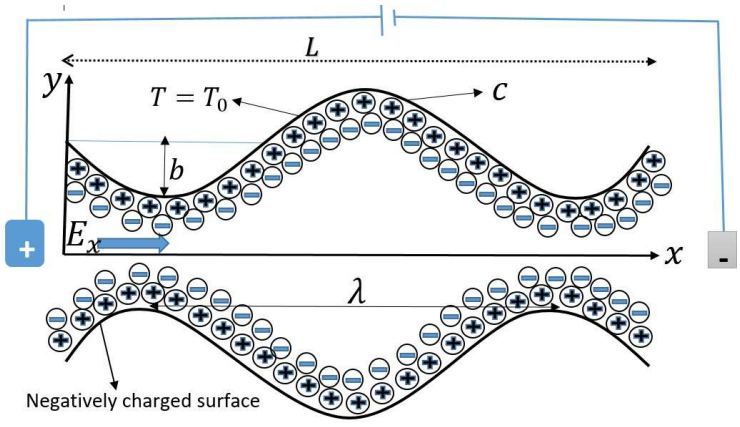

Fig. 1: Geometry of the problem.

The equation of the wall surface can be written as:

$$H(X,\bar{t}) = a + b\sin\left(\frac{2\pi}{\lambda}(X - c\bar{t})\right), \tag{2.1}$$

where λ is the wave length, $\bar{t}$ is time, a is the half of the channel width, b is the wave amplitude.

2.2 Governing Equations

A firm approach to analyze the non-Newtonian character of the fluid is the Jeffrey liquid model. For the Jeffrey fluid model, the shearing stress and shearing strain are related by the relationship as given below.

$$\bar{T} = -\bar{P}\bar{I} + \bar{S}, \tag{2.2}$$

where,

$$\bar{S} = \frac{\mu}{1+\lambda}(\dot{\gamma} + \lambda_2\ddot{\gamma}). \tag{2.3}$$

Here $\bar{T}$ represents the Cauchy stress tensor, $\bar{S}$ represents the extra stress tensor, $\bar{P}$ represents the pressure, $\bar{I}$ is the identity tensor, $\dot{\gamma}$ is the shear rate and dot over the quantities denotes differentiation.

In the laboratory frame, fundamental equations for the flow of Jeffrey fluid in electro-kinetic environment ([27], [28] and [32]) are
Continuity equation:

$$\frac{\partial \bar{w}}{\partial \bar{x}} + \frac{\partial \bar{v}}{\partial \bar{y}} = 0, \tag{2.4}$$

Momentum equations:

$$\rho\left(\bar{w}\frac{\partial \bar{w}}{\partial \bar{x}} + \bar{v}\frac{\partial \bar{w}}{\partial \bar{y}}\right) = -\frac{\partial \bar{p}}{\partial \bar{x}} + \frac{\partial S_{\bar{x}\bar{x}}}{\partial \bar{x}} + \frac{\partial S_{\bar{y}\bar{x}}}{\partial \bar{y}} + \rho_e E_{\bar{x}}, \tag{2.5}$$

$$\rho\left(\bar{w}\frac{\partial \bar{v}}{\partial \bar{x}} + \bar{v}\frac{\partial \bar{v}}{\partial \bar{y}}\right) = -\frac{\partial \bar{p}}{\partial \bar{y}} + \frac{\partial S_{\bar{y}\bar{x}}}{\partial \bar{x}} + \frac{\partial S_{\bar{y}\bar{y}}}{\partial \bar{y}}, \tag{2.6}$$

Energy equation:

$$\rho c_p\left(\bar{w}\frac{\partial \bar{T}}{\partial \bar{x}} + \bar{v}\frac{\partial \bar{T}}{\partial \bar{y}}\right) = K\left(\frac{\partial^2 \bar{T}}{\partial \bar{x}^2} + \frac{\partial^2 \bar{T}}{\partial \bar{y}^2}\right) + S_{\bar{x}\bar{x}}\frac{\partial \bar{w}}{\partial \bar{x}} + S_{\bar{y}\bar{y}}\frac{\partial \bar{v}}{\partial \bar{y}} + S_{\bar{x}\bar{y}}\left(\frac{\partial \bar{w}}{\partial \bar{y}} + \frac{\partial \bar{v}}{\partial \bar{x}}\right) + \frac{\partial}{\partial \bar{y}}(\bar{q}_r). \tag{2.7}$$

In the above equations, $\bar{w}$ and $\bar{v}$ are components of velocity in $(\bar{x},\bar{y})$ directions respectively in fixed reference frames, ρ is density, $\bar{p}$ is pressure, $\bar{T}$ is temperature, K is thermal conductivity, c_p is specific heat at constant pressure, $S_{\bar{x}\bar{x}}$, $S_{\bar{y}\bar{x}}$, $S_{\bar{y}\bar{y}}$ are stress tensor components.

2.3 Electrical Potential Distribution

From the Gauss law, we have

$$\nabla.\bar{E} = \frac{\rho_e}{\varepsilon}, \tag{2.8}$$

where,

$$\bar{E} = -\nabla.\bar{\Phi}. \tag{2.9}$$

The Poisson equation for electrical potential distribution can be described with the help of equations (2.8) and (2.9):

$$\nabla^2 \bar{\Phi} = -\frac{\rho_e}{\varepsilon} \tag{2.10}$$

In which, ρ_e and ε are the density of the total ionic energy and electric permittivity respectively. The ions and counter-ions have the equal charge valance $z_+ = z_- = z$, for a symmetric electrolyte.

Thus, the total density of the ionic charge is given by

$$\rho_e = ez(\bar{n}_+ - \bar{n}_-), \tag{2.11}$$

In which e and z stands for elementary charge and charge balance. The cations (positive) $\bar{n}_+$ and anions (negative) $\bar{n}_-$ have bulk concentration (number density). The charge number density must be determined to establish the potential distribution, making the Nernest-Plank equation useful for this endeavor. It can be described as follows [22]:

$$\frac{\partial \bar{n}_\pm}{\partial \bar{t}} + \bar{u}\frac{\partial \bar{n}_\pm}{\partial \bar{x}} + \bar{v}\frac{\partial \bar{n}_\pm}{\partial \bar{y}} = \mathbf{D}\left(\frac{\partial^2 \bar{n}_\pm}{\partial \bar{x}^2} + \bar{v}\frac{\partial^2 \bar{n}_\pm}{\partial \bar{y}^2}\right) \pm \frac{\mathbf{D}ez}{T_e K_B}\left[\frac{\partial}{\partial \bar{x}}\left(\bar{n}_\pm \frac{\partial \bar{\Phi}}{\partial \bar{x}}\right) + \frac{\partial}{\partial \bar{y}}\left(\bar{n}_\pm \frac{\partial \bar{\Phi}}{\partial \bar{y}}\right)\right], \tag{2.12}$$

Here it is presumed that for both species, the ionic diffusion coefficients are equal and that the mobility of the species is determined by the Einstein formula, where **D** is the diffusion coefficient, K_B is the Boltzmann constant, T_a is the average temperature of the electrolytic solution.

The Poisson equation is determined as follows:

$$\frac{\partial^2 \bar{\Phi}}{\partial \bar{y}^2} = -m^2\left(\frac{n_+ - n_-}{2}\right), \tag{2.13}$$

where $m = aez\sqrt{\frac{2n_0}{\varepsilon k_B T}} = \frac{a}{\lambda_d}$ is known as the Debye-Hückel parameter, λ_d is the EDL or Debye-length. Additionally, the simplified Nernst-Planck equations are intended to provide the ionic distribution:

$$\frac{\partial^2 n_\pm}{\partial \bar{y}^2} \pm \frac{\partial}{\partial \bar{y}}\left(n_\pm \frac{\partial \bar{\Phi}}{\partial \bar{y}}\right) = 0 \tag{2.14}$$

Equation (2.14) with bulk $n_\pm = 1$ at $\bar{\Phi} = 0$, $\frac{\partial n_\pm}{\partial \bar{y}} = 0$, at $\frac{\partial \bar{\Phi}}{\partial \bar{y}} = 0$, yields the Boltzmann distribution for the ions:

$$n_\pm = e^{\pm \bar{\Phi}} \tag{2.15}$$

Substituting Eq. (2.15) in to Eq. (2.14), one gets the Poisson-Boltzmann paradigm for calculating the distribution of electrical potentials

$$\frac{\partial^2 \bar{\Phi}}{\partial \bar{y}^2} = -m^2 \sinh(\bar{\Phi}) \tag{2.16}$$

Equation (2.16) has to be simplified to proceed with the analysis further. Under the Debye-Hückel's linearization (i.e., $\xi < 25mV$ over a large pH range), $\sinh(\bar{\Phi}) \approx \bar{\Phi}$. Consequently, equation (2.16) may be reduced to:

$$\frac{\partial^2 \bar{\Phi}}{\partial \bar{y}^2} = -m^2 \bar{\Phi} \tag{2.17}$$

Employing the boundary conditions $\frac{\partial \bar{\Phi}}{\partial \bar{y}} = \xi$ at $\bar{y} = 0$ and $\bar{\Phi} = 1$ at $\bar{y} = H$ to solve the equation (2.17), we get

$$\bar{\Phi} = \frac{\xi \cosh(m\bar{y})}{\cosh(mH)}. \tag{2.18}$$

2.4 Non-Dimensional, Lubrication Approach, and Boundary Conditions

The transformation between wave and the fixed frame is defined by:

$$w = \bar{w} - c, \quad v = \bar{v}, \quad x = \bar{x}, \quad y = \bar{y}. \tag{2.19}$$

The transformations used in the above equations are in scale

$$w=\frac{\bar{w}}{c}, v=\frac{\bar{v}}{c\delta}, x=\frac{\bar{x}}{\lambda}, y=\frac{\bar{y}}{a}, H=\frac{h}{a}, \delta=\frac{a}{\lambda}, p=\frac{\bar{p}a^2}{\mu c\lambda}, \Phi=\frac{\bar{\Phi}}{a}, R_e=\frac{\rho ca}{\mu}, \tag{2.20}$$

$$\theta=\frac{\bar{T}-T_0}{T_0}, U_{hs}=-\frac{E_{\bar{x}}\varepsilon\xi}{\mu c}, t=\frac{c\bar{t}}{\lambda}, pr=\frac{\mu c_p}{K}, R_d=-\frac{16\sigma\bar{T}^3}{3\kappa\mu c_f}, \ ,Br=E_c pr, E_c=\frac{c^2}{c_f(T_1-T_0)}, \phi=\frac{b}{a}.$$

In which w,x,v,y are axial velocity, axial coordinate, transverse velocity and transverse coordinates are respectively in wave frame. In Eq. (2.20) δ is the wavenumber, pr is the Prandtl number, E_c is the Eckert number, ϕ is the amplitude ratio, and $E_{\bar{x}}$ is electro kinetic force, ξ is the channel wall zeta-potential. U_{hs} is the maximum electro-osmotic velocity, respectively.

After introducing equations (2.19) and (2.20), equation (2.4), satisfies identically, and equations (2.5)-(2.8), with rearrangement the following will be produced,

$$\frac{\partial w}{\partial x}+\frac{\partial v}{\partial y}=0 \tag{2.21}$$

$$R_e\delta\left(w\frac{\partial w}{\partial x}+v\frac{\partial w}{\partial y}\right)=-\frac{\partial p}{\partial x}+\delta\frac{\partial S_{xx}}{\partial x}+\frac{\partial S_{yx}}{\partial y}+U_{hs}m^2\frac{\partial^2\Phi}{\partial y^2}, \tag{2.22}$$

$$R_e\delta^3\left(w\frac{\partial v}{\partial x}+v\frac{\partial v}{\partial y}\right)=-\frac{\partial p}{\partial y}+\delta^2\frac{\partial S_{yx}}{\partial x}+\delta\frac{\partial S_{yy}}{\partial y}, \tag{2.23}$$

$$R_e\delta^3\left(\frac{\partial\theta}{\partial x}+v\frac{\partial\theta}{\partial y}\right)=(1+prR_d)\left(\delta\frac{\partial^2\theta}{\partial x^2}+\frac{\partial^2\theta}{\partial y^2}\right)+E_c pr\left(\delta\left(S_{xx}\frac{\partial w}{\partial x}+S_{yy}\frac{\partial v}{\partial y}\right)+S_{xy}\left(\delta^2\frac{\partial v}{\partial x}+\frac{\partial w}{\partial y}\right)\right), \tag{2.24}$$

where,

$$S_{xx}=\frac{2\delta}{1+\lambda}\left[1+\frac{\lambda_2\delta c}{a}\left(w\frac{\partial}{\partial x}+v\frac{\partial}{\partial y}\right)\right]\frac{\partial v}{\partial x},$$

$$S_{xy}=\frac{2\delta}{1+\lambda}\left[1+\frac{\lambda_2\delta c}{a}\left(w\frac{\partial}{\partial x}+v\frac{\partial}{\partial y}\right)\right]\frac{\partial w}{\partial y},$$

$$S_{yy}=\frac{1}{1+\lambda}\left[1+\frac{\lambda_2\delta c}{a}\left(w\frac{\partial}{\partial x}+v\frac{\partial}{\partial y}\right)\right]\left[\frac{\partial w}{\partial y}+\delta\frac{\partial v}{\partial x}\right].$$

Using the long wavelength ($0<\lambda<\infty$) and low Reynolds number ($R_e\to 0$), and neglecting the terms of δ and higher, equations (2.21)-(2.24), reduces to

$$\frac{\partial p}{\partial x}=\left(\frac{1}{1+\lambda}\frac{\partial w}{\partial y}\right)+m^2U_{hs}\Phi, \tag{2.25}$$

$$h=1+\phi\cos(2\pi x), \tag{2.26}$$

$$\frac{\partial p}{\partial y}=0, \tag{2.27}$$

$$(1+prR_d)\frac{\partial^2\theta}{\partial y^2}=Br\frac{1}{1+\lambda}\left(\frac{\partial w}{\partial y}\right)^2, \tag{2.28}$$

where $Br=E_c pr$ is the Brinkman number.

According to Saffaman, the following boundary conditions are given:

$$\frac{\partial w}{\partial y} = 0, \text{ at } y = 0, \quad \text{and} \quad w = -1 - \frac{\sqrt{Da}}{a}\frac{\partial w}{\partial y}, \text{ at } y = h, \tag{2.29}$$

$$\frac{\partial \theta}{\partial y} = 0, \text{ at } y = 0, \quad \text{and} \quad \theta = 0 \text{ at } y = h. \tag{2.30}$$

where, Da is Darcy number and a is the slip parameter.

Volume flow rate is given by:

$$\bar{Q}(x,t) = \int_0^h (w+1)dy = q + h. \tag{2.31}$$

$$Q = \frac{1}{T}\int_0^T \bar{Q}dt = q + 1. \tag{2.32}$$

The pressure rise per wavelength is

$$\Delta p = \int_0^1 \frac{\partial p}{\partial x}dx. \tag{2.33}$$

3 Analytical Solution

Employing the boundary conditions of equation (2.29) to solve the equation (2.25), we get

$$w = -\frac{1}{2\alpha}\left(2\alpha + \frac{\partial p}{\partial x}\left(2\sqrt{Da}h + \left(h^2 - y^2\right)\alpha\right)(1+\lambda_1) + 2(1+\lambda_1)\xi U_{hs}\left(\alpha\frac{\cosh(my)}{\cosh(hm)} - \sqrt{Da}m\tanh(hm) - \alpha\right)\right) \tag{3.1}$$

From, Eq. (3.1), the pressure gradient can be obtained interims of flow rate as follows:

$$\frac{\partial p}{\partial x} = \frac{-3m(h+Q-1)\alpha + 3(1+\lambda_1)\xi U_{hs}\left(hma + \left(hm^2\sqrt{Da} - \alpha\right)\tanh(hm)\right)}{h^2 m\left(3\sqrt{Da} + h\alpha\right)(1+\lambda_1)} \tag{3.2}$$

The solution for temperature is obtained by solving Eq. (2.28) with boundary condition (2.30):

$$\theta = \frac{1}{24m^2(1+prR_d)}\left(A_1 + 3Br(1+\lambda)\xi\frac{U_{hs}A_2}{\cosh(hm)}\right), \tag{3.3}$$

where,

$$A_1 = 2m^2\left(12(1+prR_d) + Brp^2\left(h^4 - y^4\right)(1+\lambda)\right),$$
$$A_2 = 16p\left(2\cosh(hm) - A_3 + \frac{A_4 U_{hs}}{\cosh(hm)}\right),$$
$$A_3 = 2\cosh(my) - hm\sinh(hm) + my\sinh(my),$$
$$A_4 = m^2\xi\left(2m^2\left(y^2 - h^2\right) + \cosh(2hm) - \cosh(2my)\right)$$

4 Results and Discussions

The foremost aim in this article is look into the electro-kinetic flow of viscoelastic fluid in channel with permeable wall. The thermal radiation and heat effect is taken into the account. As a result, in this segment we have offered the graphical

concerns of the solutions. The terminologies for velocity, temperature and pressure gradient are premediated numerically by **Mathematica** software.

Figure 2(a) illustrates the influence of material parameter λ on velocity. An increase in the value of λ declines the magnitude of velocity. The escalation of a set of this parameter causes more resistance to the fluid flow and reduces its velocity, i.e., ratio of relaxation to retardation times (which suggests durable viscoelastic effect). Additionally, the opposite trend observed at the end of wall. Figure 2(b) is conspired to display the behavior of w under the influence of Da. Velocity has slowed up behavior in the central area of the channel while accelerating effects near the walls of the channel. The physical reason behind this phenomenon is that the resistance of fluid flow reductions as the porosity of the walls growths, leading to an augmented velocity distribution near the channel walls. The influence of electro-osmotic parameter m on axial velocity profile explicated by Fig. 2(c). It is noticed that with increasing electroosmotic parameter (i.e., for smaller Debye length) there is a substantial acceleration in the center of the channel, while with increasing m there is a substantial slowing down in the axial velocity near the channel wall. Physically, the cations and anions move in the core region to form electro-osmotic flow (EOF), which causes the axial velocity to increase. In contrast, the repulsion of positive and negative charges in the ambient layer to the walls slows down the flow, which causes the axial velocity to decrease. Figure 2(d) portrayed to demonstrates the impacts of zeta potential parameter ξ on the velocity profile w against the non-dimensional parameter y respectively. It is found that, the upsurge of the zeta potential parameter ξ decelerate the velocity profile w at the core of the channel while velocity field slightly upsurge with an increase in ξ near the channel wall. Also, the effect of ξ is found to be remarkable near the axis of the channel compared to the wall surface and the effect ceases for the threshold radius. In Fig. 2(e), we can see the variation in velocity distribution for different values of the Helmholtz-Smoluchowski parameter U_{hs}. The velocity exhibits a slowing behavior in the center area of the channel ($y = 0$), while there are accelerating effects near the walls of the channel. Therefore, the main purpose of the axial electric field is to control the flow. The Helmholtz-Smoluchowski parameter U_{hs} determines the physical decline in fluid velocity as the EDL thickness increases. Consequently, the presence of the EDL leads to a decrease in fluid flow.

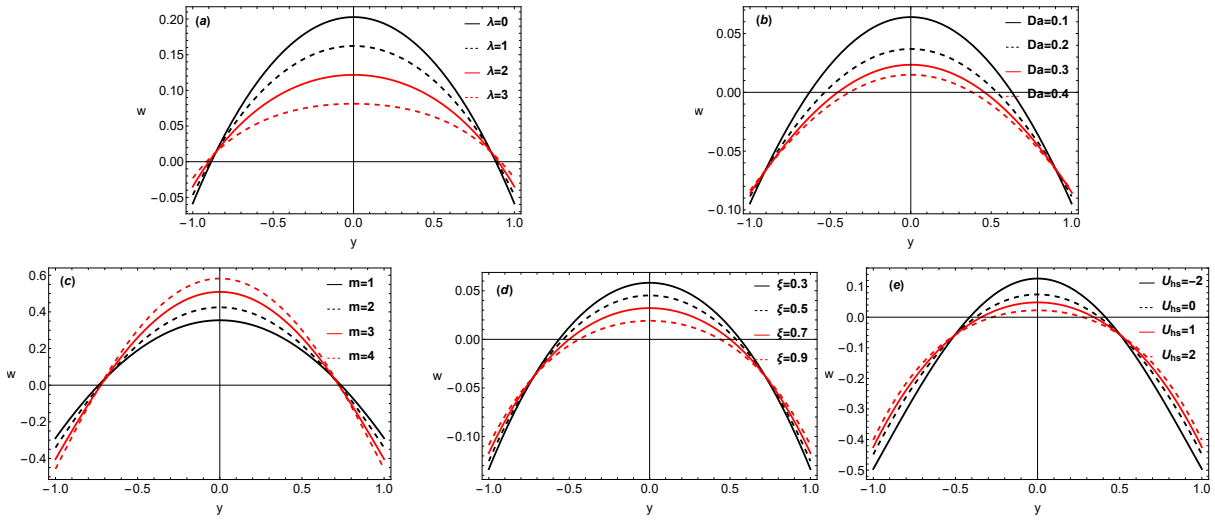

Fig. 2: The axial velocity w vs y for different values of (a) λ_1, (b) Da, (c) m, (d) ξ, and (e) U_{hs} with $\Phi = 0.6, m = 2, U_{hs} = 1, \xi = 0.1, Q = 0.9, Da = 0.01, \alpha = 0.1, \lambda_1 = 2$.

In order to gain insights into the presumed research, we will explore the impact of various constraints on temperature. Figures 3(a)-3(h) are equipped to explain the process of heat transfer in the present flow configuration. Figure 3(a) is revealed to analyze the influence of material parameter λ on θ. It is observed that the temperature profile decreases as the Jeffrey fluid parameter λ invereases. Figure 3(b) reveals that the contribution of Helmholtz- Smoluchowski velocity U_{hs} on temperature profile θ at different values of $U_{hs} = -1, 0, 1$ and 1.5. It is demonstrated that the magnitude of the temperature θ decreases with an increase in U_{hs}. This further emphasizes the influence of electric field on temperature and its role in regulating the heat transport. Figure 3(c) shows the temperature curve for different electro-osmotic parameter m values while maintaining the other parameters constant. The graph shows that as m grows, temperature reduces. This indicates that the relationship between temperature and the electro-osmotic parameter is significant in regulating the heat transfer process. Therefore, it can be concluded that the electric field plays a primary role in controlling heat transfer.

Figure 3(d) shows the changes in temperature for various values of zeta potential ξ It can be perceived from this figure that the temperature decreases with an increase in ξ. In Fig. 3(e), we witness the change in temperature distribution for different values of Brinkmann number Br. From Fig. 3(e), we noticed that temperature has accelerating behavior in the channel for different Br. Temperature increases dramatically as a result of this behavior because the greater the magnitude of the Brinkman number, the less heat conduction is produced through viscous dissipation. The influence of Prandtl number pr on temperature is shown in Fig. 3(f). It is evident from Fig. 3(f) that the Prandtl number tends to decrease the temperature in the micro-channel. It can be suggested that the thermal conductivity of the fluid decreases as the ratio of momentum diffusivity to thermal diffusivity increases. Figure 3(g) illustrates the impact of increasing thermal radiation R_d on temperature θ. It can be observed that as R_d increases, the magnitude of temperature decreases. This phenomenon can be attributed to the inverse correlation between radiation and thermal conduction.

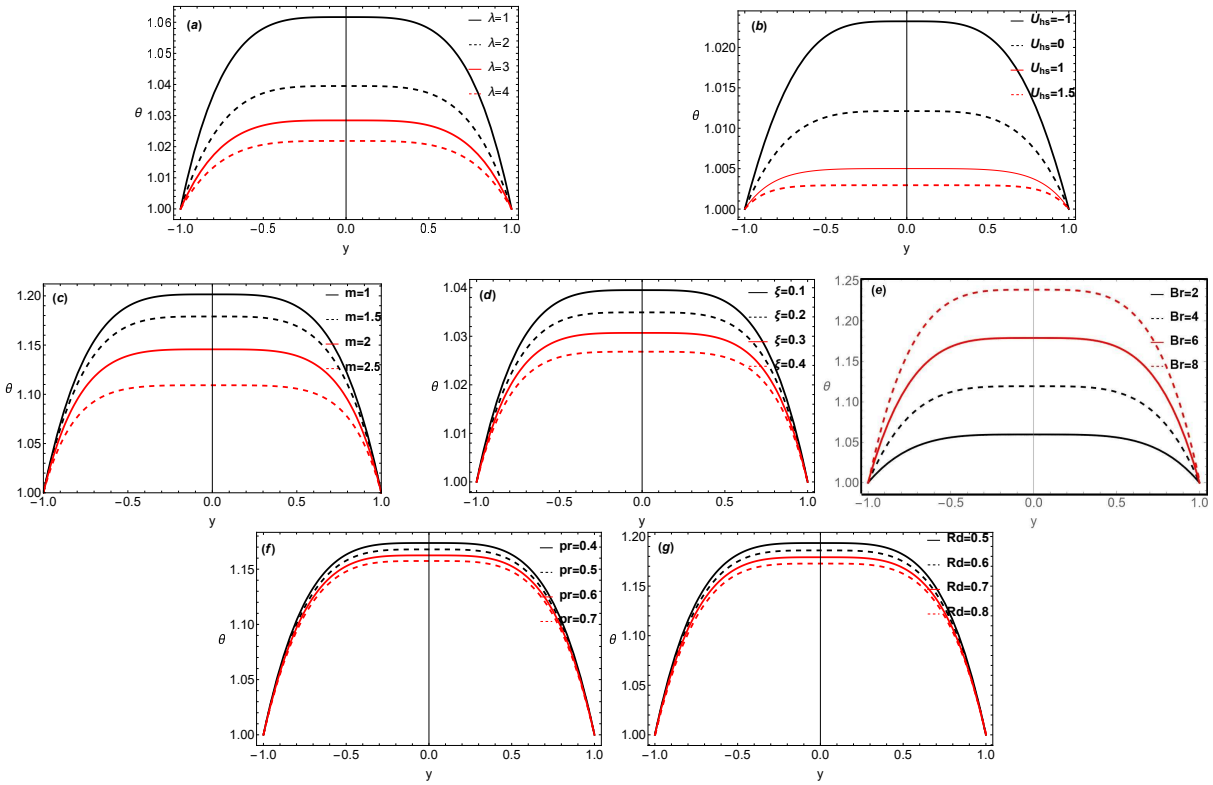

Fig. 3: The temperature θ vs y for different values of (a) λ_1, (b) U_{hs}, (c) m, (d) ξ, (e) Br (f) pr and (g) R_d with $\Phi = 0.3, m = 2, U_{hs} = 1, \xi = 0.1, Q = 0.1, Da = 0.01, \alpha = 0.1, \lambda_1 = 2, pr = 0.7, R_d = 0.4, x = 0.25$.

The influence of various features on pressure gradient is depicted in Figs. 4(a)-4(e). The distribution of $\frac{\partial p}{\partial x}$ relation to the axial coordinate (x) has been shown in Figs. 4(a)-4(e). It is evident that the axial length's pressure gradient is sinusoidal in nature, with high pressure gradients at contraction and low-pressure gradients at relaxation, which creates the peristaltic pumping process. This pumping allows for the controlled transfer of a volume of liquid from one area to another without any disturbance. The analysis of Figs. 4(a) and 4(b) reveals that the pressure gradient is insignificant for x values within the range of $[0, 0.4]$ and $[0.7, 1]$. However, a substantial pressure gradient is observed for x values within the range of $[0.4, 0.65]$. Additionally, it has been observed that an increase in the Dabey-Hückel parameter ($m = \frac{a}{\lambda_d}$), which represents the inverse thickness of the electric double layer (EDL), leads to an increase in the pressure gradient. This implies that a negative pressure gradient may occur as the thickness of the EDL decreases. From Fig. 4(b), it can be observed that the pressure gradient consistently increases with an increasing value of U_{hs}. The same trend can be observed for the increasing values of ξ, as shown in Fig. 4(c). Figures 4(d) and 4(e) represents the variation of pressure gradient $\frac{\partial p}{\partial x}$ for the impacts of material parameter λ_1 and Darcy number Da. From these two figure it is clear that the pressure gradient decelerates with an upsurge in λ and Da.

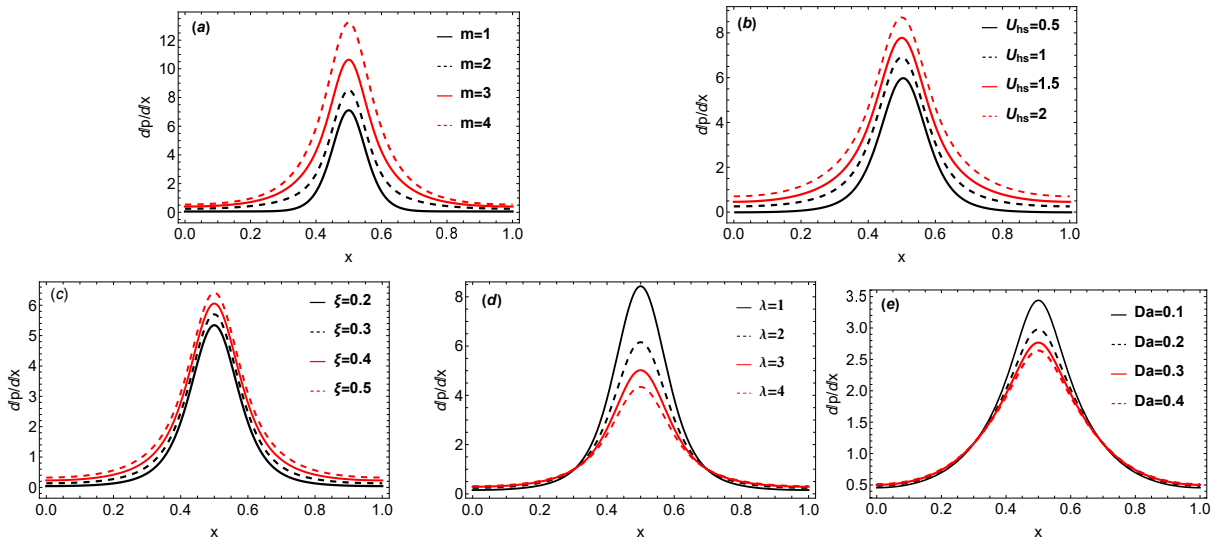

Fig. 4: The axial pressure $\frac{\partial p}{\partial x}$ vs x for different values of (a) m, (b) U_{hs}, (c) ξ, (d) λ, (e) Da with $\Phi = 0.6, m = 2, U_{hs} = 1, \xi = 0.5, Q = 0.2, Da = 0.01, \alpha = 0.1, \lambda_1 = 1, y = 0.25$.

5 Conclusions

To improve the understanding of the mechanism involved in peristaltic motion of Jeffrey fluids, this study has investigated additional factors such as electro-osmosis, thermal radiation, and heat transfer in a channel with a permeable wall. These findings provide valuable insights for improving the performance of bio-microfluidic devices that utilize electro-osmosis and peristalsis. Analytical methods have been employed to successfully address the issue at hand, offering solutions for the velocity, temperature, and pressure gradient of the fluid model under examination. Graphical representations have been used to visually illustrate the physical characteristics of the system. The main outcomes of this research can be summarized as follows:

–The velocity enhances with enhancing Helmhotz-Smoluchowski parameter U_{hs}.
–The temperature is seen to increase when Brinkmann number Br upswings.
–It is witnessed that the pressure gradient upsurges for large values of m, ξ, U_{hs}.
–It is obvious that the larger Debye-Hückel parameter significantly strengthens the temperature field near the channel core.
–It is marked that when pr and R_d rise, the temperature profile drops.
–Rise in the values of Da, and λ leads to a decline in velocity and temperature distributions.

Declarations

Competing interests: No conflict of interest.
Authors' contributions: Authors contributed equally in this manuscript.
Funding: No funding for this research.
Availability of data and materials: The data in this manuscript is open for publication.
Acknowledgments: The authors would like to thank the reviewers for their useful suggestions which helped to improve the quality of the paper.

References

[1] Y. C. Fung, C. S. Yih, Peristaltic Transport, *Journal of Applied Mechanics*, **35(4)** (1968), 669-675.
[2] A. H. Shapiro, M. Y. Jaffrin and S. L. Weinberg, Peristaltic pumping with long wavelengths at low Reynolds number, *Journal of Fluid Mechanics*, **37(4)** (1969), 799-825.

[3] T. Hayat, S. Noreen, N. Ali, S. Abbasbanday, Peristaltic motion of Pan-Thien Tanner Fluid in a planner channel, *Numerical Methods for Partial Differential Equations*, **28(3)** (2010), 738-748.
[4] V. P. Rathod, M Mahadev, A study of ureteral peristalsis with fluid flow, *Internal Journal of Mathematical Modelling, Simulation and Applications*, **5** (2012), 11-22.
[5] V. P. Rathod, M Mahadev, Interaction of heat transfer and peristaltic pumping of fractional second grade fluid through vertical cylindrical tube, *Thermal Science*, **18** (2014) 1109-1118.
[6] D. Tripathi, A mathematical model for the peristaltic flow of chime movement in small intestine, *Mathematical Bioscience*, **233** (2011), 90-97.
[7] A. Saleem, A. Qaiser, S. Nadeem, M.Ghalambaz, A. Issakhov, Physiological flow of non-Newtonian fluid with variable density inside a ciliated symmetric channel having compliant wall, *Arabian Journal for Science and Engineering*, **46** (2021), 801-812.
[8] K. Vajravelu, S. Sreenadh, S. Dhananjaya, P. Lakshminarayana, Peristaltic flow and heat transfer of a conducting Phan-Thien-Tanner fluid in an asymmetric channel-application to chyme movement in small intestine, *International Journal of Applied Mechanics and Engineering*, **21(3)** (2016), 713-736.
[9] A. Saleem, S. Akhtar, F. M. Alharbi, S. Nadeem, M. Ghalambaz, A. Issakhov, Physical aspects of peristaltic flow of hybrid nano fluid inside a curved tube having ciliated wall, *Results in Physics*, **19** (2020), 103431.
[10] V. P. Rathod, M Mahadev, Effect of thickness of porous material on the peristaltic pumping of Jeffrey fluid with non-erodible porous lining wall, *International Journal of mathematical Archive*, **2** (2011), 1-10.
[11] K. Vajravelu, G. Radhakrishnamacharya V. Radhakrishnamurty, Peristaltic flow and heat transfer in a vertical porous annulus, with long wave approximation, *International Journal of Non-Linear Mechanics*, **42** (2007), 754-759.
[12] S. Samreen, H. Sadaf, N. S. Akabar, N.A. Mir, Heat and peristaltic propagation of water-based nanoparticles with variable fluid features, *Physica Scripta*, **94** (2019), 125074.
[13] S.K Asha, C.K. Deepa, Impacts of hall and heat transfer on peristaltic blood flow of MHD Jeffrey fluid in a vertical asymmetric porous channel, *International Journal of Advances in Applied mathematics and Mechanics*, **6** (2019), 55-63.
[14] H. Sadaf, S. Nadeem, Fluid flow analysis of cilia beating in a curved channel in the presence of magnetic field and heat transfer, *Canadian Journal of Physics*, **98** (2020), 191-197.
[15] H. Sadaf, S. Nadeem, Analysis of Combined convective and viscous dissipation effects on peristaltic flow of Rabinowistch fluid model, *Journal of Bionic Engineering*, **14** (2017), 182-190.
[16] M.M. Channakote, D.V. Kalse, The consequences of wall properties and slip on the peristaltic motion of Jeffery liquid in a non-uniform tube with heat transfer, *International Journal of Creative Thoughts*, **10** (2022), 300-310.
[17] Galal M. Moatimid, Mona A. A Mohamed Khaled Elagamy, Peristaltic Rabinowistch nanofluid with moving microorganisms, *Scientific Reports*, **13** (2023), 1863.
[18] M.M. Channakote, D.V. Kalse, Heat transfer in peristaltic motion of Rabinowitsch fluid in a channel with permeable wall, *Applications and Applied Mathematics*, **16** (2021), 1057-1076.
[19] M.M. Channakote, D.V. Kalse, Combined convective and viscous dissipation effects on Peristaltic flow of Ellis fluid in a non-uniform tube, *Journal of Naval Architecture and Marine Engineering*, **19** (2022), 1-12.
[20] M.Y. Rafiq, Z.Abbas, Impact of viscous dissipation and thermal radiation on Rabinowistch fluid model Obeying peristaltic mechanism with wall properties, *Arbian Journal for Science and Engineering*, **46** (2021), 12155-12163.
[21] S.K. Asha, G. Sunitha, Thermal radiation and Hall effects on peristaltic blood flow with double diffusion in the presence of nanoparticles, *Case Studies in Thermal Engineering*, **17** (2020), 100560.
[22] T. Hayat, Saima Rani, A. Alsaedi Maimona Rafiq, Radiative Peristaltic flow of magneto nano fluid in a porous channel with thermal radiation, *Results in Physics*, **7** (2017), 3396-3407.
[23] N. Imran, M. Javed, M. Sohail, I. Tlili, Simultaneous effects of heterogeneous-homogeneous reactions in peristaltic flow comprising thermal radiation: Rabinowitsch fluid model, *Journal of Materials Research and Technology*, **9** (2020), 3520-3529.
[24] H. Sadaf, I. Shahzadi, Physiological transport of Rabinowitsch fluid model with convective conditions, *International Communications in Heat and Mass Transfer*, **126** (2021), 105365
[25] M. Kothandapani, J. Prakash, Effects of thermal radiation parameter and magnetic field on the peristaltic motion of Williamson nano fluids in a tapered asymmetric channel, *International Journal of Heat and Mass Transfer*, **81** (2015), 234-245.
[26] S. Chakraborty, Augmentation of peristaltic micro flows through electro-osmotic mechanisms, *Journal of Physics D Applied Physics*, **39** (2006), 5356.
[27] A. Mangesh, M.Kothandapani, V. Pushparaj, Electro-osmotic flow of Jeffery fluid in an asymmetric micro channel under the effect of magnetic field, *Journal of Physics Conference Series*, (2021), 1-12.
[28] K. Venugopal, Reddy, B. Venkateshwaralu, D. Channa Kesavaiah, N. Nagendra, Electroosmotic flow of Jeffrey fluid in a rotating microchannel by peristalsis: thermal analysis, *Science, Engineering and Technology*, **3(1)** (2023), 50-66.
[29] Bandopadhyay, D. Tripathi, S. Chakraborty, Electro osmosis-modulated peristaltic transport in microfluidic channels, *Physics of Fluids*, **28** (2016), 052002.
[30] D. Tripathi, Shashi Bhushan, O. Anwar Bég, Analytical study of electro-osmosis modulated capillary peristaltic hemodynamic, *Journal of Mechanics in Medicine and Biology*, **17** (2017), 1750052-12.
[31] S. Ijaz, Rafia, H. Sadaf, Electro-osmotically generalized bio-rheological fluid flowing through a ciliated passage, *Materials Science and Engineering: B*, **290** (2023), 116340.
[32] D. Tripathi, R. Jhorar, O.A. Bég, S. Shaw, Electroosmosis modulated peristaltic biorheological flow through an asymmetric microchannel : mathematical model. *Meccanica*, **53(8)** (2017) 2079-2090.

[33] S. Waheed, S. Noreen, A. Hussanan, Study of heat and mass transfer in flow of third order fluid through peristaltic micro channels, *Applied Science*, **9** (2019), 2164.
[34] J. Akram, N.S. Akbar, E.N. Maraj, A comparative study on the role of nanoparticle dispersion in electro osmosis regulated peristaltic flow of water, *Alexandria Engineering Journal*, **59(2)** (2020), 943-956.
[35] D. Tripathi, R. Jhorar, O. Anwar Bg and Sachin Shaw, Electro-osmosis modulated peristaltic bio rheological flow through an asymmetric microchannel: mathematical model, *International Journal of Theoretical and Applied Mechanics*, **53** (2018), 2079-2090.
[36] M. M Channalote, S.K. Asha, Heat transfer and electro-osmotic Analysis on peristaltic pumping of fractional second grade fluid through a cylindrical tube, *International Journal of Computational Material Science and Engineering*, **12** (2023), 235007-17.
[37] Kh.S. Mekheimer, Nonlinear peristaltic transport through a porous medium in an inclined planar channel, *Journal of Porous Media*, **6** (2003), 190-202.
[38] N. S. Akbar, M. Raza and R. Ellahi, Influence of induced magnetic field and heat flux with the suspension of carbon nanotubes for the peristaltic flow in a permeable channel, *Journal of Magnetism and Magnetic Materials*, **381** (2015), 405-4015.
[39] Kh. S. Mekheimer, B. M. Shankar, R. E. Abo-Elkhair, Effects of Hall current and permeability on the stability of peristaltic flow, *Applied Science*, **1** (2019), 610.
[40] H. Vaidya, R. Choudhari, G. Manjunath, K.V. Prasad, Effect of variable liquid properties on peristaltic transport of Rabinowistch liquid in convectively heated complaint porous channel, *Journal of Central South University*, **26** (2019), 1116-1132.
[41] N. S. Akbar, A. W. Butt, Ferromagnetic Nano model study for the peristaltic flow in a plumb duct with permeable walls, *Microsystem Technologies*, **25** (2019), 1227-1234.
[42] S. Nadeem, Iqra Shahzadi, Single wall carbon nanotube analysis on peristaltic flow in an inclined tube with permeable walls, *International Journal of Heat and Mass Transfer*, **97** (2016), 794-802.
[43] D. Tripathi, Adil Butt, O. Anwar Bég, Physical hydrodynamic propulsion model study on creeping viscous flow through a ciliated porous tube, *Pramanna Journal of Physics*, **88** (2017), 52.
[44] S. Noreen, Quratulain, D. Tripathi, Heat transfer analysis on electroosmotic pumping in non-Darcy porous medium, *Thermal Science and Engineering Progress*, **11** (2019), 254–262.